Journal of Catalysis 256 (2008) 278–286

Contents lists available at ScienceDirect

Journal of Catalysis

www.elsevier.com/locate/jcat

Defect formation and the water–gas shift reaction on β-Ga_2O_3

Wilfrid Jochum [a], Simon Penner [a], Reinhard Kramer [a], Karin Föttinger [b], Günther Rupprechter [b], Bernhard Klötzer [a,*]

[a] Institut für Physikalische Chemie, Universität Innsbruck, A-6020 Innsbruck, Austria
[b] Institut für Materialchemie, Technische Universität Wien, Veterinärplatz 1, A-1210 Wien, Austria

ARTICLE INFO

Article history:
Received 5 December 2007
Revised 20 February 2008
Accepted 21 March 2008
Available online 29 April 2008

Keywords:
β-Ga_2O_3
CO_2 adsorption
Defects
Oxygen vacancy formation
Thermal desorption spectrometry
CO adsorption
CO_2 adsorption
Water–gas shift reaction

ABSTRACT

The water–gas shift reaction was studied in either direction on β-Ga_2O_3 samples with different surface chemistries: a fully oxidized surface, a hydrogen-pretreated surface with and without oxygen vacancies present, and an oxygen-defective surface without adsorbed hydrogen. The samples were characterized by volumetric adsorption measurements and temperature-programmed desorption and reaction techniques. The reaction in both directions was observed to follow two parallel mechanistic pathways, namely formate- and oxygen vacancy-assisted mechanisms, with relative rate contributions depending on temperature and sample pretreatment.

1. Introduction

It is well known that gallium oxides and Ga-containing materials are catalytically active in a wide variety of reactions, including hydrocarbon dehydrogenation and aromatization [1–3], hydrocarbon isomerization [4], reduction of NO_x by hydrocarbons [5], methanol steam reforming [6,7], conversion of methanol to hydrocarbons [8], and carbon dioxide hydrogenation/methanol synthesis [9–11]. Different types of active Ga sites with respect to oxidation state and geometry have been postulated in the literature [2,12,13]. For Ga-doped H-ZSM5 zeolites, mobile Ga_2O species interacting with the zeolite lattice have been discussed [12]. Ga-hydride species have been identified as active species during the aromatization of light alkanes [2]. In addition, for CO_2 hydrogenation, surface hydrides $Ga^{\delta+}$–H ($\delta < 2$) are reported to play a dominant role in the formation and conversion of hydrogenated oxycarbonaceous reaction intermediates [13]. Furthermore, for the specific case of methanol steam reforming and synthesis, the exceptionally high activity of Ga_2O_3-supported Pd catalysts has been ascribed to the presence of Pd-Ga alloys forming during reductive treatments at temperatures around 523 K [6].

Because knowledge about the interaction of the reactants with the sample surface is crucial to understanding the reaction mechanism and identifying the nature of the intermediates and the catalytically active centers, numerous studies on the interaction of important probe molecules with different Ga-oxide samples have been carried out [14–21]. In terms of methanol steam reforming and synthesis, these include H_2, CO_2, CO, H_2O, and CH_3OH. A series of contributions has focused on the interaction of H_2 and CO_2 with different Ga_2O_3 polymorphs [10,11,13–16]. Regarding CO_2, after a preceding oxidation/reduction cycle, CO_2 exposure at 323 K and subsequent heating in streaming CO_2 up to 723 K was found to lead to up to six differently adsorbed carbon-oxygenate species with different binding energies as identified by in situ FTIR spectroscopy [16]. Studies on the interaction of CO with β-Ga_2O_3 and other gallia polymorphs were aimed mainly at gaining insight into the surface acidity of solid gallia-containing catalysts and CO-sensoring properties [17,18]. The interaction of H_2O with β-Ga_2O_3 surfaces was examined in depth by Meixner et al. [19], with special focus on the co-adsorption of H_2O with probe molecules relevant for the (inverse) water–gas shift reaction (WGSR), most notably H_2 and CO. A strong influence of the H_2O adsorption by formation of surface OH groups on the co-adsorption of other molecules, on the structure of the material itself, and on the catalytically active centers was observed [19]. Finally, the adsorption of CH_3OH molecules was studied in detail by Bonivardi et al. [20,21] through FTIR spectroscopy and DFT calculations. The local surface chemical composition was found to be most crucial, giving rise to three types of different adsorption pathways: nondissociative, dissociative, and oxidative decomposition [20,21].

Because the surface chemistry of β-Ga_2O_3 has been identified as the crucial parameter affecting the adsorption properties of methanol synthesis/steam-reforming reactant molecules and in-

* Corresponding author. Fax: +43 512 507 2925.
E-mail address: bernhard.kloetzer@uibk.ac.at (B. Klötzer).

0021-9517/$ – see front matter
doi:10.1016/j.jcat.2008.03.018

termediates, the present contribution provides a systematic study of the adsorption of CO_2 and CO on differently pretreated β-Ga_2O_3 samples with different surface chemistry and surface defect structures. Special attention is given to a precise quantification of the adsorbed molecules by volumetric adsorption measurements. Because the WGSR is of crucial importance in methanol synthesis/steam reforming, the influence of the surface chemistry and defect structure of β-Ga_2O_3 samples on both routes of the WGSR (i.e., $CO + H_2O$ vs $CO_2 + H_2$) is highlighted. This work builds on and extends our earlier paper dealing with H_2 and H_2O adsorption and defect formation on β-Ga_2O_3 [22].

2. Experimental

2.1. Materials

Two different β-Ga_2O_3 samples were used in this work. First, a commercial low-surface area β-Ga_2O_3 sample (99.99% purity), supplied by Alfa Aesar, was calcined in air at 1000 K. The surface area after pretreatment of the samples was determined by adsorption of nitrogen at 77 K according to BET (area, 4.0 m^2/g). In addition to the low-surface area β-Ga_2O_3 sample, a high-surface area sample was prepared by dissolution of the commercial sample using 30% aqueous NaOH in a PTFE beaker (to avoid alkaline disintegration of glass), followed by dilution with water and precipitation of crystalline $Ga(OH)_3$ at around 90 °C using an equimolar amount of ammonium nitrate (with respect to NaOH) in aqueous solution. The precipitate was thoroughly washed with hot deionized water, filtrated, and dried in air at 130 °C for 1 h. According to [18], the precipitation of a GaO(OH) containing gel from an aqueous solution followed by drying and calcination at 673 K leads to the exclusive formation of α-Ga_2O_3, which can be converted to β-Ga_2O_3 by high-temperature annealing at 1073 K for 4 h. The latter heating procedure was thus applied in air to our sample, yielding a well-ordered β-Ga_2O_3 sample with a surface area of 19.4 m^2/g. The comparable crystallographic order of both β-Ga_2O_3 samples was demonstrated by X-ray diffraction.

The "reprecipitated" ~20 m^2/g sample also was evaluated by XPS to estimate the surface-related contaminants; ⩽3% Na was found in the near-surface regions at maximum. Thus, a limited influence of near-surface Na^+ species onto the measurements presented in this work was discernible. Differences between the both samples with respect to hydrogen adsorption were rather small. The total amount of adsorbed H_2 under at the same experimental conditions was almost the same, but the reducibility of the surface to form vacancies was somewhat lower for the Na-containing high-surface area sample (cf. [22]). Nevertheless, the general trends observed on H_2 adsorption were comparable. With respect to CO_2 adsorption, the expected difference of a higher number of adsorption sites for carbonate formation was verified, as discussed in Section 2.2.

Hydrogen (5.0), helium (5.0), and oxygen (3.5) were high-grade gases supplied by Messer-Griesheim. Hydrogen was further purified by passage through an oxygen-removing purifier. Condensable contaminants were removed from hydrogen and helium by liquid nitrogen traps, whereas oxygen was passed through a trap cooled with liquid nitrogen/ethanol. CO_2 was dried by passage through a molecular sieve and a liquid nitrogen/ethanol cooling trap at 223 K.

CO (at a maximum of 200 mbar) was dried over liquid nitrogen. Mixtures for the WGSRs were always 1:1 mixtures of CO and H_2O with a total pressure of 48 mbar. For the inverse WGSRs, 1:1 mixtures of CO_2 and H_2 with a total pressure of 48 mbar also were used. These differently pretreated β-Ga_2O_3 samples were exposed to CO/H_2O and CO_2/H_2 mixtures, as outlined below.

Table 1
Defect concentration and H_2 coverage as a function of the reduction temperature and O_2 reuptake after H_2 desorption

H_2-pretreatment temperature [K]	β-Ga_2O_3 4.0 m^2/g		β-Ga_2O_3 19.4 m^2/g	
	H_2-adsorption [μmol/g]	O_2-reuptake [μmol/g]	H_2-adsorption [μmol/g]	O_2-reuptake [μmol/g]
373	0.8	0.0	3.9	0.0
473	3.3	0.0	9.7	0.0
573	5.6	0.1	21.3	0.1
673	7.0	2.4	29.1	2.0
773	7.3	5.6	31.0	9.7
873	7.1	10.4	33.0	21.3

Reduction in a flow of 1 bar dry H_2 (liquid nitrogen trap), 60 ml/min, at the respective temperature for 1 h. The defect concentration was quantified in [22] by temperature-programmed volumetric oxidation.

2.2. Volumetric apparatus

Volumetric measurements were performed in an all-glass apparatus equipped with metal bellow valves (Witeg), a Baratron pressure transducer (MKS), and mass flow controllers (MKS). To ensure volumetric measurements at temperatures of up to 1000 K, the reactor part of the apparatus containing the sample was made of quartz glass. The mass of the gallia samples was 3.1611 g for the low-surface area sample and 0.9780 g for the high-surface area sample, to provide sufficient volumetric effects in the measurements.

Pretreatment of the β-Ga_2O_3 surface was carried out in hydrogen at 298–773 K and in oxygen at 973 K at a flow rate of 1.0 mL/s. Before each oxygen treatment, the sample was evacuated at 300 K by a diffusion pump (base pressure, 5×10^{-7} mbar), heated in high-vacuum conditions to 973 K at a rate of 10 K/min (TPD measurements), and then cooled in vacuo. The oxygen uptake was measured volumetrically at 313–973 K to ensure quantitative reoxidation of gallia to its stoichiometric state.

Reactant detection was carried out by continuous mass spectrometry detection. All of the temperature-programmed CO and CO_2 reactions, as well as the (inverse) WGSR, were corrected with respect to the thermal expansion of the reaction gas mixtures, and the $m/z = 28$ CO mass spectrometry signal was corrected for the simultaneous contribution of the respective CO_2 fragment. Complete mass balance of both the WGSR and the inverse WGSR reaction routes was established by a very good agreement between the sum of the QMS-derived partial pressures of CO, CO_2, H_2, and H_2O with the simultaneously recorded total pressure at any time and reaction temperature.

3. Results and discussion

3.1. H_2 and H_2O adsorption and defect formation on β-Ga_2O_3

As outlined in a previous article on H_2 adsorption and defect formation on β-Ga_2O_3 [22], it is experimentally possible to prepare defective surfaces of β-Ga_2O_3 with and without adsorbed hydrogen (see Table 1). We particularly emphasize the importance of using dry H_2 (dried in a liquid nitrogen trap) for surface reduction and defect formation, to avoid defect quenching by heterolytic water adsorption and/or hydrolysis of H(ads) on reduced surface Ga centers. From the results in [22], it is clear that defects and H(ads) are highly sensitive to hydrolysis. We found that switching from dry H_2 to H_2 + 6.1 mbar H_2O caused the immediate quenching of defects, as demonstrated by subsequent quantitative TPO analysis. The intensity of the Ga–H infrared region (~2010 cm^{-1}) was strongly diminished in the presence of small traces of water.

By using water-free H_2, the defect concentration can be controlled via the reduction temperature and time, whereby a temperature of 550 K must be exceeded to initiate the reduction of

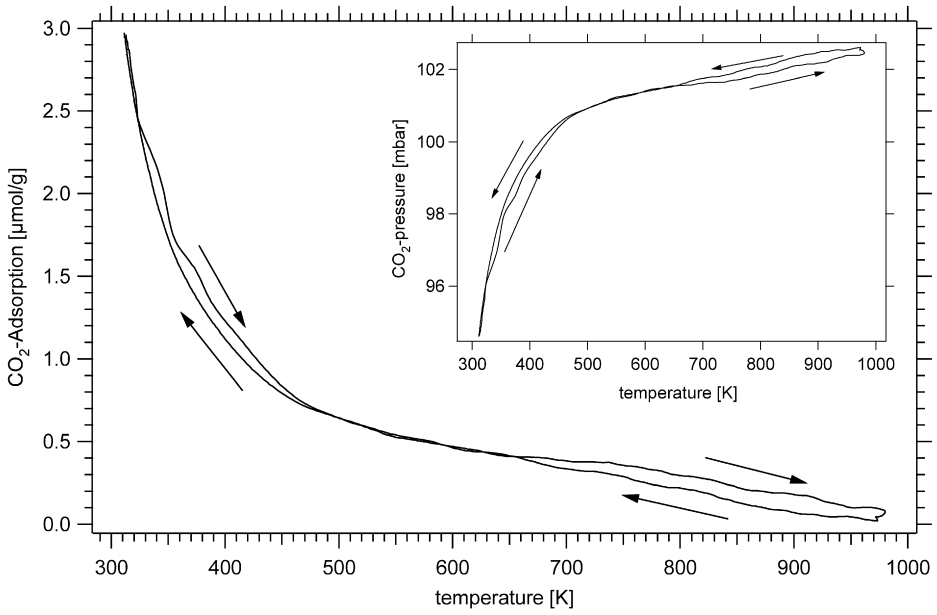

Fig. 1. Reversible CO_2-adsorption on fully oxidized β-Ga_2O_3 (4 m^2/g). Heating rate and cooling rate: 10 K/min. The highest temperature (973 K) was kept constant for 10 min. Initial equilibrium CO_2 pressure 95 mbar, for better comparison with e.g. Fig. 4 or Fig. 6 the inset shows the temperature-corrected evolution of the CO_2 pressure as a function of the reaction cell temperature.

Ga–O bonds and the removal of lattice oxygen as water, which is constantly removed by using flowing dry H_2. Thus, the defective but H(ads)-free β-Ga_2O_3 sample can be prepared by removing the remaining H(ads) via thermal desorption under high-vacuum conditions, and their H(ads)-covered counterparts can be prepared by cooling in H_2 without subsequent H_2 thermal desorption.

In summary, four different chemical states of the β-Ga_2O_3 surface can be deliberately prepared in a controlled manner to assess both the reactivity of the defects and of the adsorbed hydrogen toward CO and CO_2 independently, which are potentially important processes in the WGSR:

- The fully oxidized (stoichiometric), water-depleted surface, using dry oxygen for oxidation.
- The hydrogen-covered surface without oxygen vacancies.
- The hydrogen-covered surface with a certain number of vacancies.
- The hydrogen-free surface with a certain number of vacancies.

3.2. CO_2 adsorption

To characterize the differences in reactivity in the fully oxidized, hydrogen-free defective, and hydrogen-covered defective β-Ga_2O_3 surfaces with respect to CO_2, first the fully oxidized surface was exposed to clean, dry CO_2 in a TPR experiment. The volumetric adsorption of dry CO_2 (equilibrium pressure of about 100 mbar) on fully oxidized β-Ga_2O_3 at 313 K resulted in an adsorbed amount of 3.0 µmol CO_2/g β-Ga_2O_3 (4.0 m^2/g sample; Fig. 1). Subsequently, the sample was subjected to a heating–cooling cycle that comprised heating from 313 to 973 K (rate, 10 K/min), keeping the temperature constant at 973 K for 10 min, then cooling at a rate of −10 K/min. It was immediately seen that CO_2 desorbed during heating, and that the same amount of CO_2 readsorbed on β-Ga_2O_3 during cooling; that is, a reversible desorption and adsorption of CO_2 over the whole temperature range was observed. According to Collins et al. [16], CO_2 can adsorb in various ways on β-Ga_2O_3. The relevant species for carbonate formation from CO_2 include a weakly bound carboxylate species and monodentate, bidentate, and polydentate carbonates formed at 313 K [16]. The different processes leading to the spectroscopically identified species cannot be clearly discerned from the curves shown in Fig. 1; however, from Arrhenius plots of the low- and the high-temperature branches of the curves in Fig. 1, differently bound CO_2 species—a weakly bound, physisorbed (heat of adsorption, 10 kJ/mol) and a more strongly bound CO_2 species (heat of adsorption, 60–80 kJ/mol)—can be distinguished on the 4-m^2/g sample. It is clear that both CO_2 physisorption and carbonate formation and decay are largely reversible over the whole temperature range, because no hysteresis effects are observed. Because the variation of the total pressure CO_2 in the TPR recipient is only 95–102.5 mbar (T-uncorrected, 112 mbar), this means that the data of Fig. 1 basically can be interpreted as a close approximation of an adsorption isobar.

Additional Na-induced basic surface centers were likely responsible for the increased number of CO_2 adsorption sites forming carbonates in the 19.4-m^2/g sample. The maximum adsorbed amount of CO_2 on the high-surface area sample at 313 K in the same pressure range was 2.4 µmol/m^2, corresponding to 46 µmol/g, compared with 0.75 µmol/m^2, corresponding to 3 µmol/g, on the low-surface area sample. The isobaric adsorption of CO_2 was measured on both samples and was found to be very similar with respect to the temperature-dependent adsorption characteristics, indicating that the major difference is in the total surface density of available sites. Whether this difference is caused mainly by Na or by surface structural differences remains an open question. The heats of adsorption on the high-surface area gallia sample are nearly the same as those obtained on the 4-m^2/g sample (weakly bonded CO_2, 10 kJ/mol; strongly bonded CO_2, ∼65 kJ/mol), indicating that the Na impurities have no significant influence on the qualitative binding behavior of CO_2.

To further clarify the WGSR mechanism, TPD of CO_2 experiments were carried out on four differently prepared β-Ga_2O_3 surfaces: surfaces prereduced at 473 and 673 K (i.e., no oxygen vacancies vs vacancy formation), each modified or not modified by adsorbed hydrogen (Fig. 2). Generally, after each pretreatment, CO_2 was exposed for 30 min at 313 K resulting in an equilibrium pressure of approximately 100 mbar CO_2. Subsequently, high vacuum was applied to the samples to remove the weakly bound (physisorbed) CO_2. Thus, subsequent TPD only revealed the more strongly adsorbed chemisorbed species that remained adsorbed in

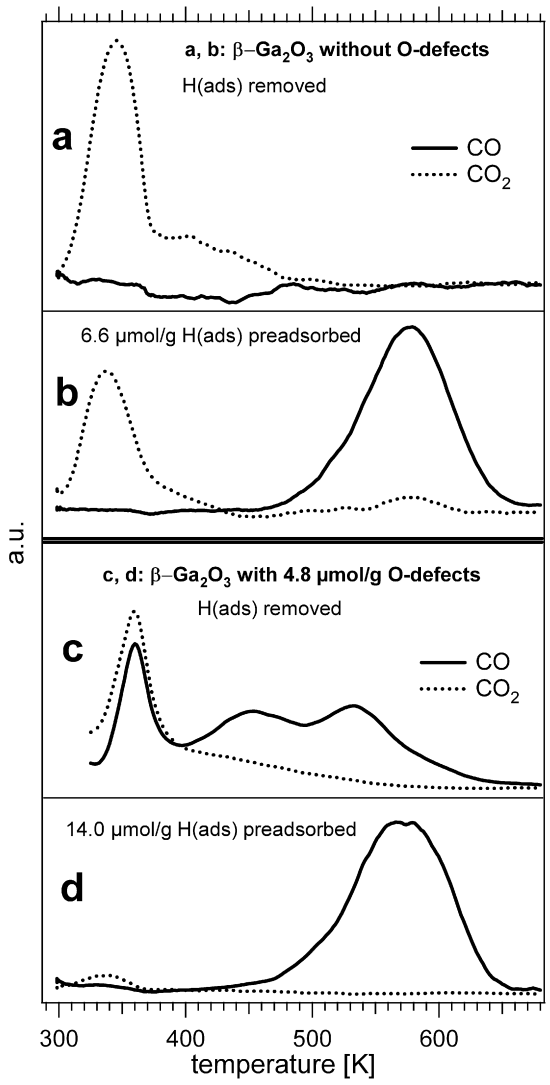

Fig. 2. TPD spectra of CO and CO_2 obtained after CO_2-adsorption on prereduced β-Ga_2O_3 (4 m^2/g): (a) and (b) prereduced at 473 K (i.e. without oxygen defects), (c) and (d) prereduced at 673 K (i.e. 4.8 µmol/g oxygen vacancies present). (a) Without oxygen defects and without H(ads), (b) without oxygen defects but with 6.6 µmol/g H(ads) preadsorbed. Full lines: CO traces, dashed lines: CO_2 traces. (c) With oxygen defects but without H(ads), (d) with oxygen defects and with 14.0 µmol/g H(ads) preadsorbed. Full lines: CO traces, dashed lines: CO_2 traces.

vacuo at 313 K. The TPD experiment included a linear temperature ramp from 313 to 973 K at a rate of 10 K/min. Figs. 2a and 2b show the respective CO_2 and CO-TPD curves without oxygen vacancies present, that is, after prereduction at 473 K for 1 h, followed either by cooling in H_2 to 313 K and high vacuum for 20 min at 313 K [H(ads) present; Fig. 2b] or by heating in high vacuum up to 973 K at a rate of 10 K/min, followed by cooling in high vacuum to 313 K [H(ads) removed; Fig. 2a]. The respective defect and hydrogen surface concentrations can be deduced from Table 1. According to [22] and Table 1, the desorption of hydrogen from the vacancy-free sample prepared at 473 K eventually resulted in the reestablishment of the initial fully oxidized surface state without oxygen vacancies.

Exposure of dry CO_2 after removal of H(ads) at 313 K resulted in CO_2 adsorption of 2.9 µmol/g. According to the subsequent TPD spectra (indicated by the dashed line in Fig. 2a), CO_2 was the only desorption product, and only formation/thermal decomposition of carbonate species (i.e., the same behavior as seen on the original, fully oxidized β-Ga_2O_3 system) was observed.

An oxygen vacancy-free surface with 6.6 µmol H(ads)/g was prepared by a H_2 pretreatment at 473 K for 1 h, followed by cooling in H_2 to 313 K and high-vacuum exposure for 20 min before admission of dry CO_2 (Fig. 2b). According to [14] (see Fig. 5) and [22], after H_2 reduction at 473 K, both the presence of homolytically adsorbed H_2 on terminal oxygen species as –OH and the partial formation of Ga–H species via heterolytic H_2 adsorption [14] (with both types adsorbed on the vacancy-free surface) was observed. Adsorption of dry CO_2 at 313 K onto this surface resulted in 1.1 µmol/g of adsorbed CO_2. In the respective TPD (indicated by the solid line in Fig. 2b), a CO-peak with a maximum at about 580 K was observed, indicating that part of the adsorbed CO_2 was able to react with H(ads) in the absence of oxygen defects directly after adsorption or during the subsequent temperature ramp of the TPD experiment. As we explain later in the context of Fig. 6, the interaction of reactive Ga–H groups on this surface most likely led to the formation of formate species, which could subsequently react toward CO and adsorbed –OH groups. The formation of bidentate HCOO species from H_2 and CO_2 at temperatures above 450 K and their decay at temperatures above 550 K have been reported by Collins et al. [11]. This mechanism, termed the "formate mechanism" in what follows, may be active in either direction, depending on the initially established surface and reaction conditions. A CO_2 peak observed in the low-temperature region around 350 K indicates that the part of the CO_2 that was not converted to CO was adsorbed as a rather weakly bound carbonate species.

Figs. 2c and 2d show the TPD spectra from the surface preparations with 4.8 µmol/g of oxygen vacancies present. Without H(ads) (after desorption of H_2 under high-vacuum conditions at 673 K and subsequent heating in high vacuum up to 973 K with +10 K/min, followed by cooling down in high-vacuum to 313 K), exposure of dry CO_2 at 313 K led to adsorption of 3.2 µmol/g of CO_2 at 313 K (Fig. 2c). In the subsequent TPD spectra, desorption of both CO_2 and CO in the low-temperature region at around 350 K was observed. First, a CO_2 peak in the low-temperature region around 350 K indicates that the part of the CO_2 that was not converted to CO was again adsorbed as a rather weakly bound carbonate species. Second, the observation of a series of CO desorption maxima (starting at ~350 K) means that β-Ga_2O_3 modified with O-vacancies was able to react with CO_2 toward CO at slightly above room temperature, leading to partial quenching of oxygen defects. Apparently, three different CO-binding states were generated through this quenching process, which obviously does not require adsorbed hydrogen-containing species, such as formate.

The last case that we evaluated involves the adsorption and reaction of CO_2 on a β-Ga_2O_3 with both oxygen vacancies and H(ads) present, prepared as outlined earlier (Fig. 2d). Exposing this surface to dry CO_2 at 313 K resulted in the adsorption of 1.1 µmol/g of CO_2. A large CO peak with a maximum at about 570 K was observed, very similar to the CO peak resulting from the H(ads)-covered surface without defects (Fig. 2b, solid line). Only very little desorption of CO_2 stemmed from some residual carbonates, in contrast to the situation for the H(ads)-covered surface without defects, on which a considerably larger CO_2 peak was observed in the TPD spectra. This finding indicates a more complete conversion of CO_2 toward CO compared with the initial state without vacancies but otherwise a similar situation involving surface formates, with most of the desorbed CO apparently resulting from formate decomposition.

In summary, compared with reversible CO_2 adsorption as carbonates on a fully oxidized surface, the situation changed drastically if the initial state of the surface was oxygen-defective and/or hydrogen-covered. In accordance with [11], H(ads) is expected to react with CO_2 toward formate species (essentially bridged bidentate HCOO), which decay toward CO and surface OH groups at temperatures above 550 K, as evidenced by the predominant CO formation shown in Fig. 2. Even more active for reductive CO_2 ac-

tivation are the "hydrogen-free" oxygen vacancies, which enable CO formation in the low-temperature region ($T > 300$ K). In all cases shown in Fig. 2, at least a small part of the CO_2 was adsorbed in the carbonate form, leading to a CO_2-TPD feature with a rate maximum around 350 K.

The smallest CO_2 contribution, as well as the complete absence of low-temperature (<400 K) CO desorption features, was observed on the sample with H(ads)-blocked vacancies (which may alternatively be denoted as cus Ga–H sites); see Fig. 2d. It is likely that this sample did not allow for a direct reaction of residual H(ads)-free vacancies with CO_2, because these sites were largely blocked by H(ads). Only the hydrogen-depleted sample, exhibiting an equivalent amount of cus Ga sites without H(ads), could effectively create the weakly bonded CO shown in Fig. 2c. From Fig. 2, it appears that all kinds of Ga–H species (i.e., cus Ga–H from homolytically adsorbed hydrogen at cus Ga sites and/or also Ga–H resulting from heterolytic H_2 adsorption without vacancies, see [22]) tended to produce formate in the presence of CO_2.

From previous measurements [22], we cannot determine whether the oxygen vacancies created during reductive pretreatment were actually quantitatively occupied by H(ads) or whether some of them remained free cus Ga sites. But comparing Figs. 2c and 2d seems to indicate that the cus Ga sites were largely H(ads)-blocked before CO_2 exposure in Fig. 2d.

Two possible explanations exist for the very small amount of carbonate-related CO_2 in remaining in the sample shown in Fig. 2d: (a) more efficient site blocking for carbonate formation, caused by the much higher total H(ads) coverage on this sample (total hydrogen surface concentration, 14 μmol/g), and (b) more efficient conversion of intermediate carbonates toward formate species due to the higher amount of coadsorbed hydrogen at or slightly above room temperature. Support for either possibility comes from the CO_2 adsorption on the low-surface area gallia sample at around room temperature; at 313 K, on the fully oxidized, H(ads)-free surface, 3.0 μmol/g CO_2 adsorbed, whereas on the 14 μmol/g H(ads)-precovered surface, only ~1.1 μmol/g CO_2 adsorbed. Therefore, a combination of partial blocking of reversible carbonatic CO_2 adsorption sites H(ads) and efficient conversion of the intermediately adsorbed CO_2 (e.g., as weakly bonded carbonate species) toward formate species (equally blocking sites) appears likely. The finding that Fig. 2d shows almost quantitatively CO and that Fig. 2b also shows some remaining CO_2 still bonded as carbonate thus likely can be explained by the higher total hydrogen surface concentration on the initially present vacancy + H(ads) sample (14 μmol/g in Fig. 2d vs 6.6 μmol/g in Fig. 2b), that is, more efficient conversion toward formate and/or site blocking. Based on our own experiments, we cannot distinguish between the surface reaction of adsorbed hydrogen with particular intermediate carbonates and/or the (unlikely) direct reaction of CO_2(g) with the Ga–H reactive sites. Rather, according to [11], it seems that the major part of the carbonate species are first decomposed and/or converted toward formate at temperatures up to 450 K. Our TPD spectra given in Fig. 2 also show that most of the carbonates were desorbed up to this temperature. A simplified picture can be suggested in which the intermediate surface concentration of weakly bonded carbonates is high at low temperatures (<350 K) and the conversion toward formate species remains slow at these temperatures. A temperature rise to above 400 K increases the decomposition of the intermediate carbonate species as well as the rate of conversion to formate; that is, their presence in the spectra is strongly diminished. However, even at a low steady-state coverage, these species may represent the dominant kinetic intermediate from CO_2 and H(ads) toward formate. The reaction scheme shown in Fig. 5 does not differentiate these different mechanisms and thus does not include the potential carbonate intermediate.

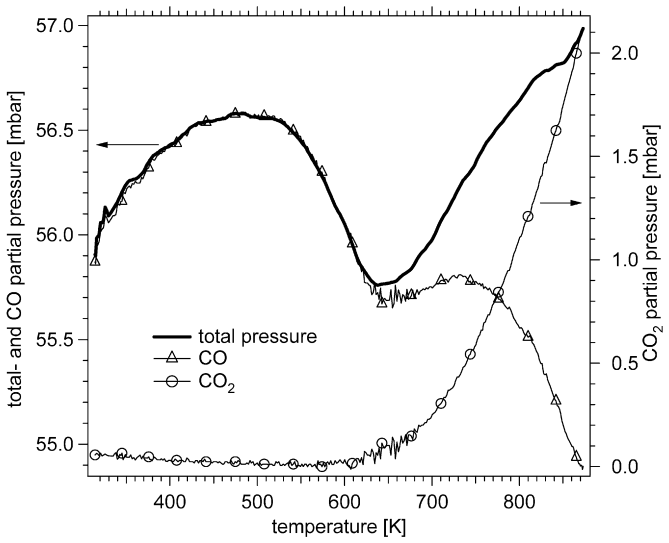

Fig. 3. CO-TPR on water-free β-Ga_2O_3 (19.4 m^2/g). Initial CO pressure ~56 mbar. Heating rate: 10 K/min.

3.3. CO adsorption and reaction

Because dry CO_2 is capable of quenching oxygen vacancies in the absence of water or surface OH species, we anticipated that the reverse process—defect formation using dry CO—also should be feasible. The TPR of initially fully oxidized β-Ga_2O_3 with dry CO is shown in Fig. 3. The preceding volumetric CO adsorption was carried out at 313 K on the fully oxidized β-Ga_2O_3 (19.4 m^2/g), resulting in an equilibrium pressure of about 56 mbar CO and 1.5 μmol/g of adsorbed CO. Then the sample was heated to 973 K (heating rate, 10 K/min). During heating between 300 and 500 K, weakly (obviously molecularly) bonded CO desorbed. Starting at ~500 K, CO adsorbed again due to a surface reaction consuming CO. This reaction most likely created reactively adsorbed CO products at reduced Ga centers. Because at above 500 K, adsorption of CO occurred without simultaneous CO_2 formation in the gas phase, we conclude that the CO remained in this strongly chemisorbed state, possibly carbonate species close to oxygen vacancies, up to 630 K, at which point CO_2 desorption started by decomposition of this state. Once CO_2 desorbed to the gas phase, oxygen vacancies necessarily remained on the surface. This experiment proves that a second reaction mechanism for the WGSR is feasible above 630 K; we call this the "vacancy-mediated" mechanism. This mechanism involves formation of defects through simultaneous CO and CO_2 formation and the continuous reoxidation of these defects by water, inducing H_2 production through a full catalytic cycle.

3.4. (Inverse) WGSR

Finally, the temperature-dependent progress of both the inverse WGSR and the WGSR were investigated through TPR experiments in either direction. To assess the influence of the initial surface state, identical TPR runs were started from the fully oxidized, hydrogen-covered, and vacancy-modified surfaces without H(ads) (Figs. 4A–4C). The reactivity-versus-temperature plot starting from the H(ads)-covered but vacancy-free surface turned out to be very similar to that highlighted in Fig. 4B [H(ads) + vacancies] and thus is not shown. This is likely because only the initial presence of vacancies without H(ads) allowed for direct interaction of some of the CO_2 with these (already at around 300 K) to form weakly bonded CO desorbing at low temperatures (i.e., <400 K; see Fig. 2c); if H(ads) were initially covering the vacancies, then

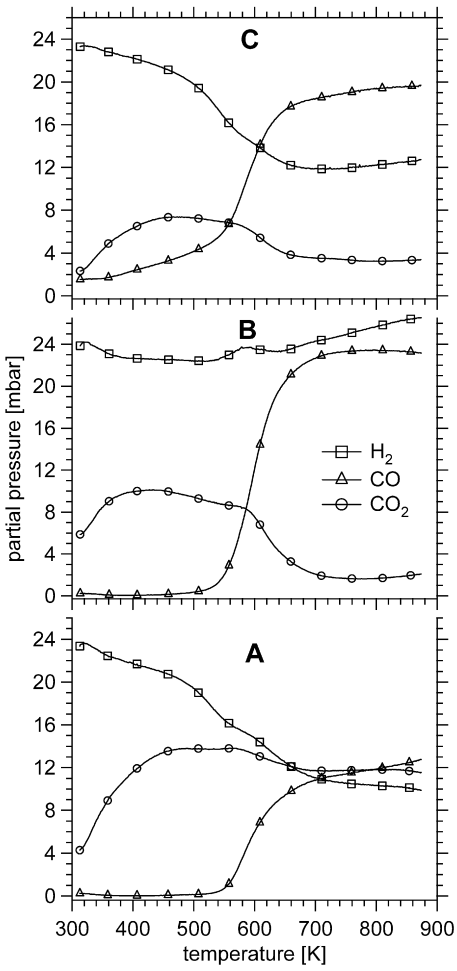

Fig. 4. Inverse WGSR activity as a function of temperature on β-Ga_2O_3 (0.978 g of the 19.4 m^2/g sample). (A) Adsorption of a 1:1 CO_2/H_2-mixture on fully oxidized β-Ga_2O_3 at 313 K. The total amount of introduced gas was 48 mbar at 313 K, whereby 20.5 mbar gas was adsorbed already at 313 K, mostly CO_2. (B) Same mixture adsorbed at 313 K onto the 773 K hydrogen-covered defective sample (64 μmol/g H(ads) + 20.6 μmol/g O-vacancies) at 313 K. Total amount of introduced reactant gas 48 mbar, 18 mbar gas adsorbed at 313 K, mostly CO_2. (C) Same mixture adsorbed at 313 K onto 773 K prereduced and hydrogen-desorbed β-Ga_2O_3 sample, i.e. with an initial defect concentration of 20.6 μmol/g O-vacancies. Total amount of introduced gas mixture again 48 mbar at 313 K, 21 mbar gas adsorbed, mainly CO_2. The water signal was not included due to detection- and quantification problems. Linear heating ramp: 10 K/min.

this direct CO_2 activation at defects toward CO obviously would be blocked (see Fig. 2d).

In Fig. 4A, the temperature-programmed inverse WGSR was performed directly after adsorption of a 1:1 CO_2:H_2 reaction mixture onto the fully oxidized β-Ga_2O_3 at 313 K, by heating to 873 K at a constant rate of 10 K/min. The major part of the introduced CO_2 was initially adsorbed at 313 K (24 mbar dosed, ∼4 mbar remaining in the gas phase), and hardly any H_2 was adsorbed (23.5 mbar remaining). This finding can be explained by results of our group demonstrating that H_2 adsorption below 730 K is an activated process [22], in contrast to CO_2 adsorption (see Fig. 1). During heating from 313 K to slightly below 450 K, no formation of CO was observed, but a combination of activated hydrogen adsorption (decreasing H_2 pressure) and desorption of weakly bound CO_2 (increasing CO_2 pressure between 313 and 450 K) was seen.

The more weakly bound fraction of the carbonate species, according to [16], is likely to desorb up to a maximum of 500 K, as also can be deduced from Figs. 1 and 4. In fact, an increase in CO_2 pressure and a decrease in hydrogen pressure were found to occur only up to ∼450 K. According to [11], the conversion of adsorbed CO_2 and hydrogen toward a bridge-bonded formate species (designated bidentate HCOO in [11]) occurred at around this temperature. Accordingly, the decreasing trend of the H_2 pressure grew stronger, due to simultaneous consumption by adsorption and bidentate HCOO formation. The CO_2 pressure remained almost constant above 450 K, due to rate-balancing between consumption toward formate and desorption.

At around 550 K, the rate of CO formation increased steeply. Obviously, at this temperature, an additional process set in, leading to both increased CO_2 consumption and pronounced CO formation. It appears that at above 550 K, an additional decrease of the hydrogen pressure occurred by consumption through the reaction

$$CO_2 + H_2 \rightleftarrows CO + H_2O.$$

At 550 K, two effects were noted that have been previously described in the literature [11,22]: the onset of oxygen defect formation through hydrogen surface reduction and the formation of major amounts of bidentate HCOO species on the surface, resulting from simultaneous exposure to CO_2 and H_2 (see Fig. 5 in Ref. [11]). Of course, the onset of oxygen vacancy formation implies the possibility that the CO_2 was readily activated at these vacancies and reacted toward CO by quenching them, a process that starts temperatures below 400 K (cf. Fig. 2c, the reaction of CO_2 with hydrogen-free defects). Based on the information available so far, two distinct reaction mechanisms for the inverse WGSR (and, conversely, the WGSR; see Fig. 6) can be formulated: the formate mechanism (FM) and the vacancy-mediated mechanism (VMM). The latter is apparently a Mars-van Krevelen-type mechanism [23]. These two alternative mechanisms are depicted in Fig. 5 as operating in parallel, with temperature-variable contributions to the overall conversion.

Which mechanism is then more likely to contribute to the rate increase observed in Fig. 4A at temperatures above 550 K? According to Fig. 5, the first step of the inverse WGSR is the same for both mechanisms—homolytic hydrogen adsorption followed by heterolytic hydrogen adsorption at the surface. From the experiments shown in [22] and in Table 1 of this work, we know that hydrogen is adsorbed without defect formation at temperatures below 550 K and that measurable amounts of oxygen vacancies are formed above this temperature. These are highly active in CO_2 activation and formation of CO via defect quenching, a process that occurs with dry CO_2 (cf. Fig. 2). The CO TPD spectra in Fig. 2 show that the main part of this “defect-generated” CO in fact desorbs at 550 K and below; therefore, we may conclude that, in principle, CO formed through the VMM can contribute to the increased inverse WGS reaction rate observed at temperatures above 550 K.

On the other hand, a certain contribution of the FM cannot be excluded, according to the IR spectra obtained on β-Ga_2O_3 in a H_2–CO_2 reaction mixture by Collins et al. The relevant set of spectra in [11] shows that the bidentate HCOO intensity (with this species verified by a control experiment on our sample, to connect to these measurements) increases up to ∼550 K but decreases thereafter, indicating thermal decomposition of the bidentate HCOO species to CO and OH(ads), as reported in [11]. The fact that the nondefective H(ads)-covered surface yielded a large amount of CO from CO_2 at around 570 K (see Fig. 2) suggests extensive decomposition of the formates toward CO.

Fig. 4B shows the course of the inverse WGSR reaction starting from the hydrogen-covered defective surface. In analogy to the situation depicted for case A, initially little H_2 but most of the CO_2 was adsorbed, for the reasons discussed previously. The H_2 partial pressure remained high throughout the entire experiment, due to the absence of H_2 consumption by activated adsorption or, conversely, initial surface saturation with H(ads). Above 550 K, the inverse WGSR set in, exactly at the same temperature as in case A.

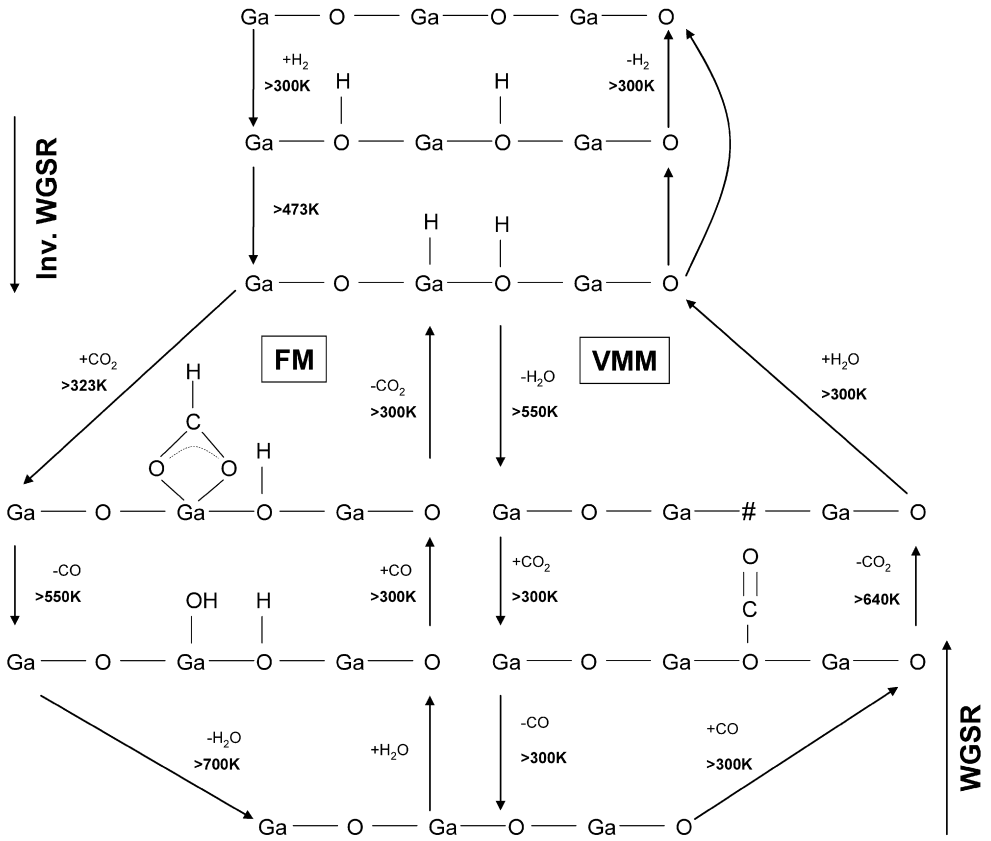

Fig. 5. Scheme of the (inverse) water–gas shift reaction on β-Ga_2O_3 proceeding along the formate-mediated (FM) and the vacancy-mediated (VMM) mechanism.

The difference is a higher degree of conversion from CO_2 toward CO, most likely because of a shift of the final equilibrium state toward CO induced by the higher H_2 pressure available. Qualitatively, the same mechanistic concepts can be assumed for both cases A and B. The initial presence of defects did not alter the reaction mechanism fundamentally, and both the FM (leading to CO at around 570 K according to Fig. 2) and the VMM (leading to H_2-induced vacancy formation above 550 K and their simultaneous CO_2 quenching) may have been operating simultaneously at around 550 K. As tested separately, after every inverse WGSR run, all oxygen vacancies were quenched, and no TPO consumption of O_2 was observed.

Finally, case C (inverse WGSR started from the defective but hydrogen-free surface) showed a nice additional rate contribution toward CO in the low-temperature region from 313 to 550 K. As already discussed in the context of Fig. 2, defects accessible to CO_2 without co-adsorbed hydrogen-induced CO formation in a much broader temperature range, 330–600 K. As suggested in the lower right side of the reaction scheme shown in Fig. 5, it appears that some CO_2 was readily adsorbed and converted to the already discussed "reactively adsorbed CO" = "carbonate at vacancy" species (depending on the viewpoint chosen!) before blocking by H(ads) occurred. This may be explained by the previously mentioned activated H_2 adsorption, which hardly occurred at 313 K. In earlier work [22], we showed that up to 730 K, H_2 adsorption was kinetically hindered and that at ~300 K, only a very small fraction of the H_2 adsorbed. Fig. 2 shows that such "carbonates at defect" species decomposed to CO at above 340 K, meaning that in this direction the VMM was hardly activated but the initial formation of defects by H_2 (at above 550 K) was rate-determining. Conversely, the rate-determining step of the FM in the inverse WGSR direction was the final water desorption step from surface –OH groups, requiring temperatures above 700 K, as can be deduced from TPD spectra involving water detection (not shown).

In the WGSR experiments illustrated in Fig. 6, we introduced a stoichiometric (1:1) amount of CO and water into the TPR cell and performed a TPR run between 313 and 873 K at a constant heating rate of 10 K/min. At 313 K, almost all of the water introduced was initially adsorbed on the β-Ga_2O_3 (19.4 m^2/g) sample, but only a minor fraction of the CO was adsorbed. The water partial pressure signal is not shown in Fig. 6, due to experimental difficulties in quantifying the true water pressure in the TPR cell by mass spectrometry. In fact, no significant water intensity could be detected in the beginning of the TPR run, that is, directly after adsorption of the reactant mixture and before the temperature ramp. The CO signal was already high at the beginning due to minor CO adsorption, and it increased only slightly with temperature due to some minor desorption effects up to the temperature of onset of the catalytic conversion (~630 K).

The CO_2 partial pressure curves in Figs. 6A and 6B reveal two distinct CO_2 formation processes: a low-temperature process that occurs without parallel hydrogen formation and thus can be interpreted as noncatalytic (at temperatures up to ~630 K) and a second, faster process with simultaneous formation of CO_2 and H_2 starting above 630 K, representing the onset of the catalytic reaction (i.e., the stoichiometric conversion of water and CO),

$$CO + H_2O \rightleftarrows CO_2 + H_2.$$

The first process is much more pronounced in Fig. 6B; that is, the initial presence of "hydrogen-free" oxygen defects induced enhanced formation of CO_2 already at lower temperatures (>350 K, in contrast to >480 K in Fig. 6B). This result appears to be surprising in view of the initially more reduced state of the catalyst of Fig. 6B; but in this context, it is useful to reconsider the TPD

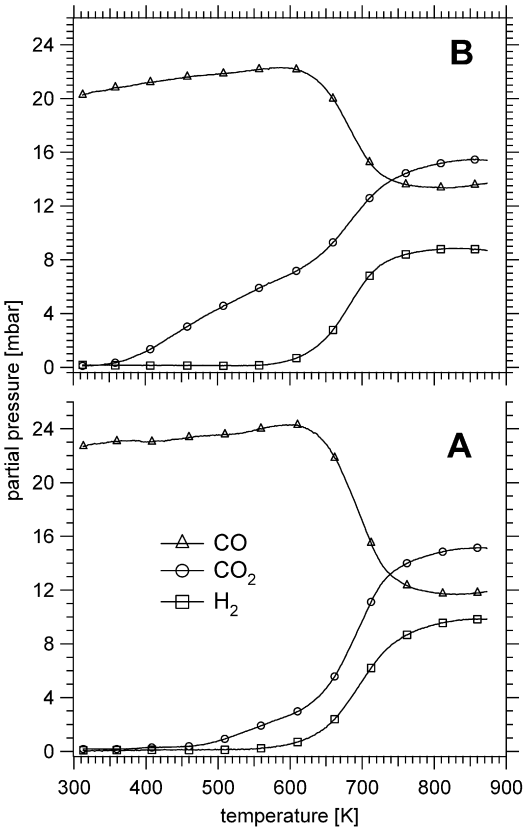

Fig. 6. WGSR activity as a function of temperature on β-Ga_2O_3 (0.978 g of the 19.4 m^2/g sample). (A) Adsorption of a 1:1 CO-H_2O-mixture (sequentially, together 48 mbar gas in the reaction cell at 313 K) on fully oxidized β-Ga_2O_3 at 313 K. 25 mbar gas become immediately adsorbed at 313 K. All H_2O is adsorbed, but only a small fraction of CO. (B) Adsorption of a 1:1 CO/H_2O-mixture on defective β-Ga_2O_3 (19.4 m^2/g, prereduced at 773 K and H(ads) thermally desorbed leading to ∼21 μmol/g hydrogen-free O-vacancies) at 313 K. Total amount of adsorbed CO/H_2O-mixture again 48 mbar, whereby 28 mbar gas become initially adsorbed. All H_2O is adsorbed, but only a small fraction of CO. The H_2O signal was not included due to detection- and quantification problems. Linear heating ramp: 10 K/min.

results presented in Fig. 2 after adsorption of CO_2 onto a hydrogen-reduced catalyst.

If the hydrogen was desorbed after reduction in the usual way ("hydrogen-free defects"), then CO_2 adsorbed at room temperature desorbed at temperatures up to 450 K as both CO and CO_2 at an approximate 1:1 ratio (Fig. 2c), whereas the hydrogen-precovered catalyst demonstrated hardly any CO desorption and some CO_2 desorption in the same temperature range (Fig. 2d). In general, the data in Fig. 2 show a considerably higher fraction of CO_2 desorbing below 450 K and a much larger fraction of CO desorbing above 450 K, even in the complete absence of water.

Of course, the major difference between the experiments shown in Figs. 2 and 6 is the simultaneous presence of CO and H_2O on the catalyst surfaces in the experiment shown in Fig. 6. As discussed in the previous section and in [22], H_2O is capable of partially re-oxidizing reduced β-Ga_2O_3 already at 313 K [22], whereby oxygen vacancy quenching creates a small fraction of gaseous H_2 and most likely a major fraction of heterolytically adsorbed water (i.e., –OH groups) at the initially present vacancy sites. Therefore, it can be safely assumed that the propensity of this water-quenched surface for CO_2- rather than CO-desorption at temperatures below 450 K would be even higher than that of a hydrogen-terminated but water-free surface. Provided that the initial presence of defects promoted heterolytic water adsorption, a larger amount of –OH groups also could be formed on the surface at close to room temperature. We propose that these groups are particularly active for CO binding and conversion toward CO_2 at above 300 K via the FM (i.e., the WGSR direction; see the left side of Fig. 5).

This mechanism, which is apparently noncatalytic in Fig. 6 (because no H_2 is formed up to 570 K), will continuously increase the hydrogen surface coverage and the CO_2 gas-phase pressure until the desorption temperature of H_2 is reached. Comparing the hydrogen evolution curves of Figs. 6A and 6B shows that H_2 desorption began at 570–580 K in both cases, irrespective of the initial surface state, meaning that above this temperature, in principle, the FM could become catalytic. The marked additional increase in the CO_2 partial pressure slope observed above 630 K indicates an additional rate enhancement, which we assign to additional defect formation by the direct reaction of CO with lattice oxygen, according to the interpretation of Fig. 3, where at above ∼630 K, CO began to reduce the β-Ga_2O_3 in a direct reaction channel (also in the absence of H_2O/OH). Necessarily, consumption of CO from the gas phase also started above 630 K. Therefore, it appears that above 630 K, two different reaction channels for CO_2 formation were active simultaneously, with the low-temperature FM being overtaken at above 630 K by the probably more strongly activated VMM.

Applying the same concept to Fig. 6A (i.e., the fully oxidized initial state), the only difference is the smaller contribution of the low-temperature FM mechanism, starting in A at above 450 K. We can tentatively attribute this difference to the less efficient heterolytic water activation on the initially fully oxidized surface, leading to formation of fewer reactive OH groups at higher temperatures. The onset of H_2 desorption and CO-induced defect formation were observed at the same temperatures in the experiments shown in Figs. 6A and 6B.

After all WGSR runs, all of the initially present oxygen vacancies were quenched, and no measurable O_2 reuptake was observed. Because the vacancy quenching process was active already at ∼300 K, we can conclude that most of the quenching occurred between 300 and 600 K, leading to the aforementioned hydroxyl species, and, therefore, the initial defect concentration had no effect on the mechanism at temperatures above 630 K mechanism.

Nevertheless, we consider the WGSR reaction at above 630 K a truly cyclic catalytic process, because oxygen vacancies are continuously formed with CO to yield CO_2 and are quenched by water to yield hydrogen, leading eventually to a rather low stationary concentration of oxygen vacancies. The initially preformed defects influence only the "noncatalytic" part of the surface reaction at the lower temperatures (e.g., if they decompose a part of the water to form OH groups, which then can react with CO). In this case, the conversion of reactants/formation of products is no longer stoichiometric, and we consider this a noncatalytic surface reaction closely related to the "true" catalytic WGSR.

4. Conclusion

Our conclusions refer directly to the optimum attainable selectivity of the methanol steam-reforming reaction toward CO_2 and H_2 as a function of temperature on Ga_2O_3-supported catalysts. The mechanistic basis for considerations related to the selective reformation on Ga_2O_3 and Pd/Ga_2O_3 has been provided by the work of Collins et al. on the intermediates of methanol synthesis from carbon dioxide and hydrogen [11], which also describes the reverse process, according to the principle of microscopic reversibility. We may first address the question why the temperature-dependent balance of the WGSR and methanol steam-reforming reaction is so important to catalytic selectivity. According to our work, temperatures of at least 600 K are needed to catalyze the equilibration of the (inverse) WGSR at a high rate on pure Ga_2O_3, and thus, in principle, a high selectivity for the CO_2–methanol pathway can

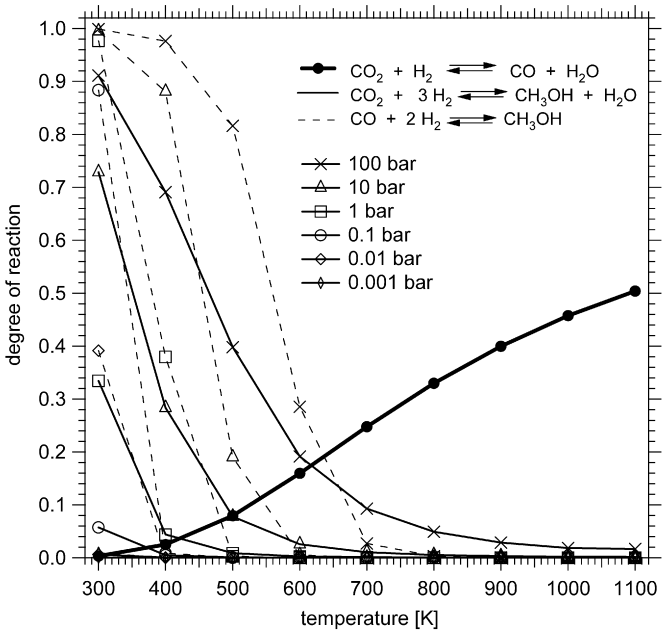

Fig. 7. Pressure-dependent reaction equilibria for three important reactions $CO_2 + H_2 \rightleftarrows CO + H_2O$, $CO_2 + 3H_2 \rightleftarrows CH_3OH + H_2O$ and $CO + 2H_2O \rightleftarrows CH_3OH$, calculated from the respective thermodynamic data in [24].

be attained at lower temperatures without major CO formation via the WGSR equilibrium.

Fig. 7 displays the calculated equilibrium degree of reaction of WGSR, methanol synthesis/steam reforming, and CO hydrogenation/methanol dehydrogenation as a function of temperature and total pressure, as calculated from the respective thermodynamic data derived from [24] (not considering fugacities and condensation effects). From this figure, it is obvious that from a thermodynamic standpoint, in principle the reaction degree of the methanol steam reforming process can reach almost 100% in the low-pressure range (maximum 100 mbar) and at temperatures above 400 K. Iwasa et al. [6] examined methanol steam reforming toward CO_2 and H_2 over $PdGa_x/Ga_2O_3$ at pressures around 100 mbar and a maximum temperature of ~500 K (well below 600 K) and found a very high selectivity toward CO_2 (~95%, i.e., only 5% CO at maximum) [6]. According to the results of our present study, we suggest that efficient catalytic equilibration of the WGSR on the clean β-Ga_2O_3 support occurred above 600 K, whereby CO formation likely proceeded through the FM and VMM mechanisms, with relative contributions depending on the reaction temperature, and could induce up to 20% CO at around 600 K (see Fig. 7).

References

[1] I. Takahara, M. Saito, M. Inaba, K. Murata, Catal. Lett. 96 (2004) 29.
[2] G.D. Meitzner, E. Iglesia, J.E. Baumgartner, E.S. Huang, J. Catal. 140 (1993) 209.
[3] I. Nowak, J. Quartararo, E.G. Derouane, J.C. Vedrine, Appl. Catal. A 251 (1) (2003) 107.
[4] J.A. Moreno, G. Poncelet, J. Catal. 203 (2001) 453.
[5] K. Shimizu, A. Satsuma, T. Hattori, Appl. Catal. B 16 (1998) 319.
[6] N. Iwasa, T. Mayanagi, N. Ogawa, K. Sakata, N. Takezawa, Catal. Lett. 54 (1998) 119.
[7] N. Iwasa, T. Mayanagi, W. Nomura, M. Arai, N. Takezawa, Appl. Catal. A 248 (2003) 153.
[8] D. Freeman, R.P.K. Wells, G.J. Hutchings, J. Catal. 205 (2002) 358.
[9] T. Fujitani, M. Saito, Y. Kanai, T. Watanabe, J. Nakamura, T. Uchijima, Appl. Catal. A 125 (1995) L199.
[10] A.L. Bonivardi, D.L. Chiavassa, C. Querini, M.A. Baltanas, Stud. Surf. Sci. Catal. 130D (2000) 3747.
[11] S.E. Collins, M.A. Baltanas, A.L. Bonivardi, J. Catal. 226 (2004) 410.
[12] P. Meriaudeau, C. Naccache, Appl. Catal. 73 (1991) L13.
[13] S.E. Collins, M.L. Baltanas, J.L. Garcia Fierro, A.L. Bonivardi, J. Catal. 211 (2002) 252.
[14] S.E. Collins, M.A. Baltanas, A.L. Bonivardi, Langmuir 21 (2005) 962.
[15] E.A. Gonzalez, P.V. Jasen, A. Juan, S.E. Collins, M.A. Baltanas, A.L. Bonivardi, Surf. Sci. 575 (2005) 171.
[16] S.E. Collins, M.A. Baltanas, A.L. Bonivardi, J. Phys. Chem. 110 (2006) 5498.
[17] T. Schwebel, M. Fleischer, H. Meixner, C.-D. Kohl, Sens. Actuators B 49 (1998) 46.
[18] M. Rodriguez Delgado, C. Otero Arean, Z. Anorg. Allg. Chem. 631 (2005) 2115.
[19] F. Reti, M. Fleischer, H. Meixner, J. Giber, Sens. Actuators B 18–19 (1994) 138.
[20] M.M. Branda, S.E. Collins, N.J. Castellani, M.A. Baltanas, A.L. Bonivardi, J. Phys. Chem. B 110 (2006) 11847.
[21] S.E. Collins, M.A. Baltanas, A.L. Bonivardi, Appl. Catal. A 295 (2005) 126.
[22] W. Jochum, S. Penner, K. Föttinger, R. Kramer, G. Rupprechter, B. Klötzer, J. Catal. (2008), doi: 10.1016/j.jcat.2008.03.019, in press.
[23] P. Mars, D.W. van Krevelen, Chem. Eng. Sci. 3 (1954) 41.
[24] I. Barin, Thermodynamic Data of Pure Substances, VCH, Weinheim, 1993.